

'Click' synthesized sterol-based cationic lipids as gene carriers, and the effect of skeletons and headgroups on gene delivery



Ruilong Sheng, Ting Luo, Hui Li, Jingjing Sun, Zhao Wang, Amin Cao*

Laboratory for Polymer Materials, Shanghai Institute of Organic Chemistry, Chinese Academy of Sciences, 345 Lingling Road, Shanghai 200032, China

ARTICLE INFO

Article history:

Received 18 June 2013

Revised 15 August 2013

Accepted 24 August 2013

Available online 3 September 2013

Keywords:

Click reaction

Sterol

Structure–activity relationships

Gene delivery

ABSTRACT

In this work, we have successfully prepared a series of new sterol-based cationic lipids (**1–4**) via an efficient 'Click' chemistry approach. The pDNA binding affinity of these lipids was examined by EB displacement and agarose-gel retardant assay. The average particle sizes and surface charges of the sterol-based cationic lipids/pDNA lipoplexes were analyzed by dynamic laser light scattering instrument (DLS), and the morphologies of the lipoplexes were observed by atomic force microscopy (AFM). The cytotoxicity of the lipids were examined by MTT and LDH assay, and the gene transfection efficiencies of these lipid carriers were investigated by luciferase gene transfection assay in various cell lines. In addition, the intracellular uptake and trafficking/localization behavior of the Cy3-DNA loaded lipoplexes were preliminarily studied by fluorescence microscopy. The results demonstrated that the pDNA loading capacity, lipoplex particle size, zeta potential and morphology of the sterol lipids/pDNA lipoplexes depended largely on the molecular structure factors including sterol-skeletons and headgroups. Furthermore, the sterol-based lipids showed quite different cytotoxicity and gene transfection efficacy in A549 and HeLa cells. Interestingly, it was found that the cholesterol-bearing lipids **1** and **2** showed 7–10⁴ times higher transfection capability than their lithocholate-bearing counterparts **3** and **4** in A549 and HeLa cell lines, suggested that the gene transfection capacity strongly relied on the structure of sterol skeletons. Moreover, the study on the structure–activity relationships of these sterol-based cationic lipid gene carriers provided a possible approach for developing low cytotoxic and high efficient lipid gene carriers by selecting suitable sterol hydrophobes and cationic headgroups.

© 2013 Elsevier Ltd. All rights reserved.

1. Introduction

Developing new cationic lipids as non-viral gene carriers for the delivery of therapeutic genes (DNA, oligo DNA, siRNA, etc.) had been achieved increasing attention in the past few decades.^{1,2} A preferred lipid gene carrier should be highly biocompatible,³ and could efficiently transport therapeutic genes⁴ into target cells to express functional proteins for disease treatment. Prior works revealed that the biological manners/behaviors of lipid gene carriers largely relied on their molecular architectures including hydrophobic moieties,^{5,6} cationic headgroups^{7,8} as well as linkers.^{9–11} Considering the profound impact of molecular structure on the safety and efficacy of lipid gene carriers, it is important to expand the structural diversity/variety of the cationic lipids and to further elucidate their structure–activity relationships towards the rational design of low toxic and high efficient lipid gene carriers. Therefore, developing modular, efficient and facile strategies or tactics for the preparation/modification of new lipid gene carriers were in high demand.

Cu⁺-mediated azide/alkyne 1,3-dipolar cycloaddition (CuAAC) reaction so-called 'Click' reaction, was considered a convenient, efficient and green synthetic method and one of the most powerful tools in chemical synthesis. In a typical 'Click' reaction, an azide-containing organic moiety reacted with an alkyne-containing moiety under the catalysis of monovalent copper (Cu⁺), resulted in the formation of triazole ring¹² by which the two moieties connected together. To date, 'Click' reaction has been widely applied in many realms such as synthesis of organic molecules,^{13,14} functional conjugation on polymers^{15–17} and materials,^{18,19} as well as non-damage labeling of living cells.^{20,21} Recently, several lipid amphiphiles have been synthesized from modular functional building blocks/moieties via 'Click' reaction. Driscoll and co-workers²² synthesized several 'Click'-modified cationic cyclodextrins as gene vectors and studied their neuronal siRNA delivery properties, and Smith et al efficiently synthesized some cholesterol–dendritic polyamine conjugates as degradable self-assembly dendrons by 'Click' method²³ and investigated their gene binding affinity, transfection performance and intracellular uptake capacity. These works demonstrated that 'Click' chemistry could be used as a promising tool for developing new functional cationic lipids as gene carriers.

* Corresponding author. Tel./fax: +86 21 5492 5303.

E-mail address: acao@mail.sioc.ac.cn (A. Cao).

On the other hand, sterols were known as natural-based lipids that played vital roles including membrane formation, hormone metabolism and cell signal transduction in organelles. Many of them possessed special features such as hydrophobicity, rigidity, mesogenic behaviors and so on, which made them functional building blocks in the construction of supramolecular architectures²⁴ and soft materials.²⁵ Recently, some steroidal compounds (such as cholesterol and cholic acid²⁶) have been utilized to construct functional gene/drug carriers. Since Huang²⁷ first reported that cholesterol derived cationic lipids could be utilized as non-viral gene carriers in 1991, up to now, many cholesterol-based cationic lipids have been synthesized and utilized as efficient gene carriers. Wolff and co-workers²⁸ connected imidazole moiety to cholesterol to prepare liposome with ‘proton buffering’ effect for efficient gene transfer. Miller and co-workers²⁹ found that a combination of cholesterol polyamine (CDAN) and DOPE could improve the stability of the lipoplex. Kim and co-workers³⁰ investigated the effect of the trimethylamine headgroup and spacer structures on gene delivery. Zenkova and co-workers³¹ revealed that some cholesterol cationic lipids modified with pyridine and methyl imidazole headgroups could gain low cytotoxicity and high transfection efficacy, similar properties could also be found on some glucosidal-modified cholesterol cationic lipids.³² Bhattacharya et al.^{33,34} developed a series of ether-containing cholesterol lipids as efficient gene carriers and studied their impact on the gene transfection efficiency. Besides, some cholesterol–dendrimer conjugates or cholesterol-hybridized lipids were also developed and proved to be efficient gene carriers. For instance, Smith and co-workers³⁵ prepared some cholesterol–dendritic polyamine conjugates and found the synergistic effects of the cholesterol moieties could play vital roles in their apparent pDNA binding capacities. Rana and co-workers³⁶ found cholesterol-hybridized cationic lipids would reduce the toxic effects of lipid-mediated siRNA delivery. Yang and co-workers³⁷ synthesized some cholesterol–conjugated amphiphilic oligopeptides (HR-Chol), which could reach 95% GFP gene transfection capacity, much higher than that of bPEI-25K in HepG2 cells. Moreover, some bio-reduction-responsive cholesterol-based gene carriers were developed. In our earlier work, we prepared a series of disulfide-bearing cholesterol cationic lipids (CHOSS),³⁸ which possessed low cytotoxicity and high gene transfection efficiencies, and an interesting perinuclear localization effect of its Cy3-pDNA payload. Recently, we found the self-assembly and transfection behaviors of some cholesterol cationic lipids could be controlled by tuning the types of cationic headgroups. However, although many cholesterol lipid gene carriers were developed, the structural dependence of their self-assembly and biological properties was not well known yet. On the other hand, the sterol family involved hundreds of molecular members, apart from cholesterol, lithocholic acid, bile acids and their derivatives were essential natural steroidal compounds, some of them were recently developed as cationic ‘molecular umbrella’^{39,40} for in vitro gene transfection. However, many cationic steroidal lipids were prepared through tedious synthetic procedures, which would hamper their further chemical modification or optimization. Moreover, elucidation of structure–activity relationships (SAR) is essential to rational design of new sterol-based cationic lipids, in prior works, Gruneich et al.^{41,42} studied the SAR between the hydrophobicity of lipid moiety of some sterol-based cationic lipids and the resultant lipofection activity. However, up to now, for most of the synthesized sterol-based cationic lipids, their SAR were still far from systematic elucidation. Additionally, the biological-related manners of many sterol-based cationic lipids, including cytotoxicity, transgene capability and intracellular trafficking/localization were not very clear so far.

In this work, we designed and synthesized a series of new cholesterol and lithocholate derived cationic lipids (**1–4**) with similar molecular building blocks, in which hydrophobic sterols were

connected with cationic headgroups via ‘Click’ reaction method. These cationic lipids showed high pDNA binding/loading affinities examined by agarose gel retardant assays, the nanoparticle sizes, surface potentials and morphologies of these sterol cationic lipids/pDNA lipoplexes were investigated by dynamic laser light scattering (DLS) and atomic force microscopy (AFM). The cytotoxicities of these newly synthesized lipids were evaluated by a thiazoyl blue tetrazolium bromide (MTT) method, and the gene transfection efficiencies of them were investigated by Luciferase assay in various cell lines. Finally, the intracellular uptake, trafficking/localization of the sterol lipids/Cy3-labeled pDNA payloads were observed and recorded by fluorescent microscopy.

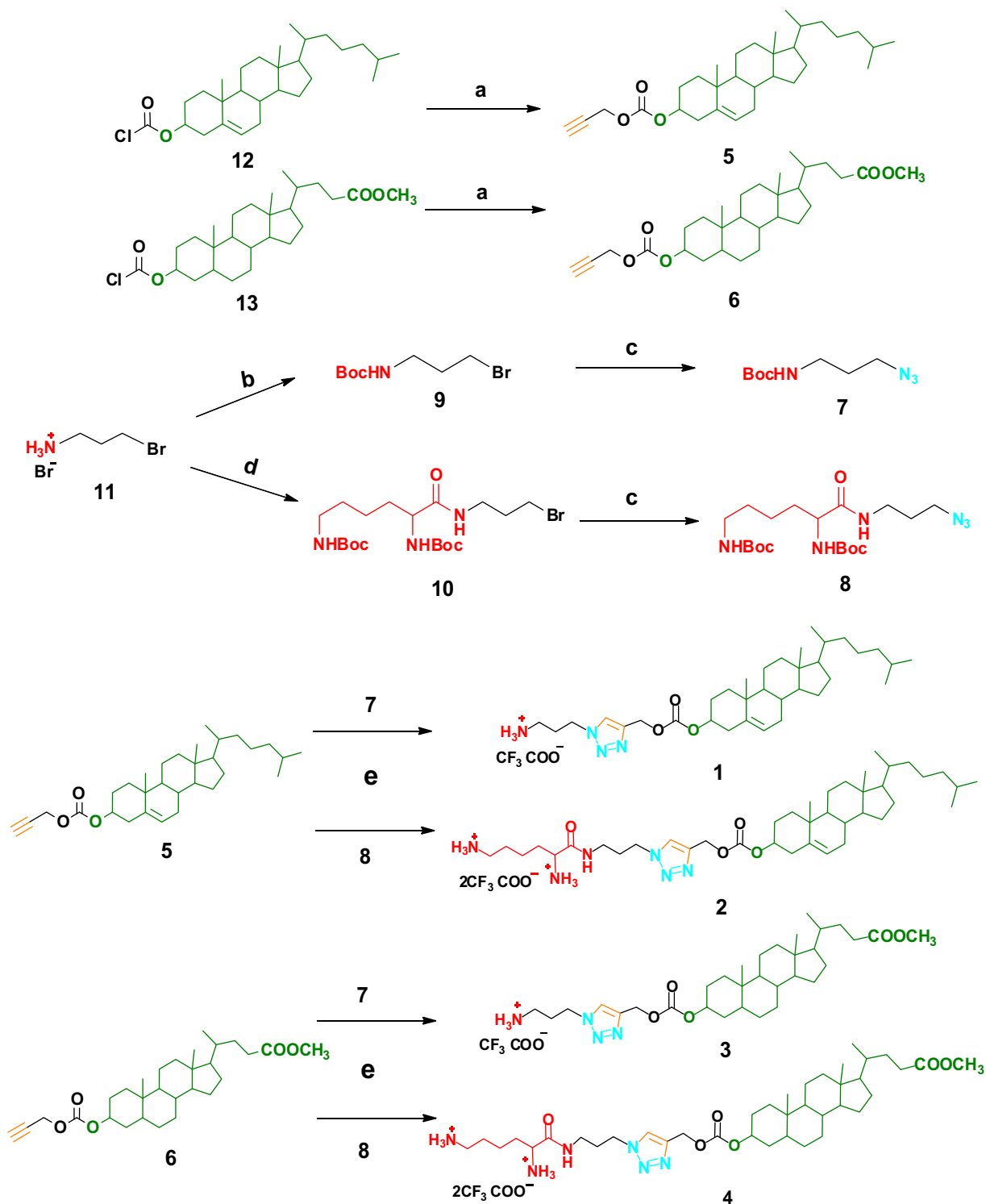
2. Results and discussion

2.1. Synthesis of the sterol-based cationic lipids

‘Click’ chemistry (CuAAC) was considered as a valuable tool for the facile connection of versatile alkynyl-bearing and azido-bearing molecular blocks at ambient reaction conditions, it offered a promising way to prepare molecular analogs with structural diversity from various modular building blocks via a combinatorial approach.⁴³ Herein, four sterol-based cationic lipids (**1–4**) were synthesized by coupling of alkynyl-bearing sterol hydrophobes with azide-bearing building blocks via CuAAC ‘Click’ chemistry. The synthetic routes were described in Scheme 1. Firstly, alkynyl-bearing sterol hydrophobes (**5** and **6**) were synthesized by coupling of cholesterol chloroformate **12** and methyl lithocholate chloroformate **13** with propargyl alcohol. Secondly, the azide-bearing building blocks (**7** and **8**) were prepared via an azido-substitution reaction using sodium azide (NaN₃) as a nucleophile and two Bromo-bearing compounds (**9** and **10**) as the precursors, and **9** and **10** were synthesized from a starting material 3-Bromo-1-propamine (**11**) through acylation on amino groups by using Boc₂O and Boc-(*l*)-lysine as the acylating agents, respectively. Then the as-prepared alkynyl-bearing sterol hydrophobes (**5** and **6**) were separately connected with azide-bearing building blocks (**7** and **8**) to form Boc-protected sterol-based cationic lipids via ‘Click’ reaction, in which Cu(I) catalyst was in situ prepared by reduction of CuSO₄·5H₂O with sodium ascorbate in aqueous solution.⁴⁴ After that, Boc protection groups were removed in the presence of trifluoroacetic acid to afford four sterol-based cationic lipids, which included two cholesterol-based cationic lipids (**1** and **2**) and two lithocholate-based lipids (**3** and **4**) as the final products with the isolation yields of 62–79%. The structural elucidation of each sterol-based cationic lipid by NMR and ESI-MS was described in detail in the experimental part, and the ¹H NMR spectra of these sterol-based cationic lipids were shown in Figure 1. The proton signal around 8.2 ppm could be identified as the protons on the newly formed triazole rings, and the proton signal at 5.1 ppm inferred the attached –CH₂– groups. Meanwhile, two obvious proton signal peaked at 8.4 and 7.8 ppm were observed on the lipids **2** and **4**, which were attributed to the α (at 7.4 ppm) and ω (at 8.4 ppm) amino groups on (*l*)-lysine headgroups. Moreover, a singlet signal at 5.3 ppm (proton on the double bond of cholesterol) could be observed on the cholesterol-bearing lipids **1** and **2**, whereas the lithocholate-containing lipids **3** and **4** did not show such signal. These results demonstrate that the new sterol-based cationic lipids **1–4** were successfully and efficiently prepared via ‘Click’ chemistry approaches.

2.2. pDNA binding of sterol-based cationic lipids

pDNA binding affinities of the sterol-based cationic lipids were evaluated by EB displacement assay and agarose gel DNA-retardation assay. As shown in Figure 2, the fluorescence intensity of the



Scheme 1. Synthetic routes and molecular structures of steroid-based cationic lipids. Reagents and conditions: (a) propargyl alcohol, CH₂Cl₂/pyridine, rt, 12 h; (b) Boc₂O anhydride, Na₂CO₃, rt, 6 h; (c) NaN₃, DMF, 80 °C, 8 h; (d) Boc-*L*-lysine, EDC-HCl/DMAP, CH₂Cl₂, rt, 24 h; (e) (1) CuSO₄·5H₂O/sodium ascorbate, THF/H₂O, 80 °C, 2 h; (2) trifluoroacetic acid, CH₂Cl₂, rt, 1 h.

pDNA/EB dye mixed solution decreased to 28–34% upon addition of monoamine headgroup bearing lipids **1** and **3** at the +/- charge ratio of 4–6, while the fluorescence intensity almost completely quenched with the addition of (*L*)-lysine (diamine) headgroup bearing lipids **2** and **4** at a higher +/- charge ratio of 2–4, indicated diamine headgroup bearing lipids tended to bind pDNA more tightly than their monoamine counterparts, due to their relatively

stronger positive-negative charge interactions with pDNA.⁴⁵ The pDNA binding affinities of the newly synthesized lipids were also studied by agarose gel DNA-retardation assay in the presence of 10 mM PBS in TAE buffer solution, as shown in Figure 3, the intensity of the migrating free pDNA bands were found decreases gradually with the increasing amount of sterol-based cationic lipids. It could be clear seen that the lipids **2** and **4** could retard pDNA

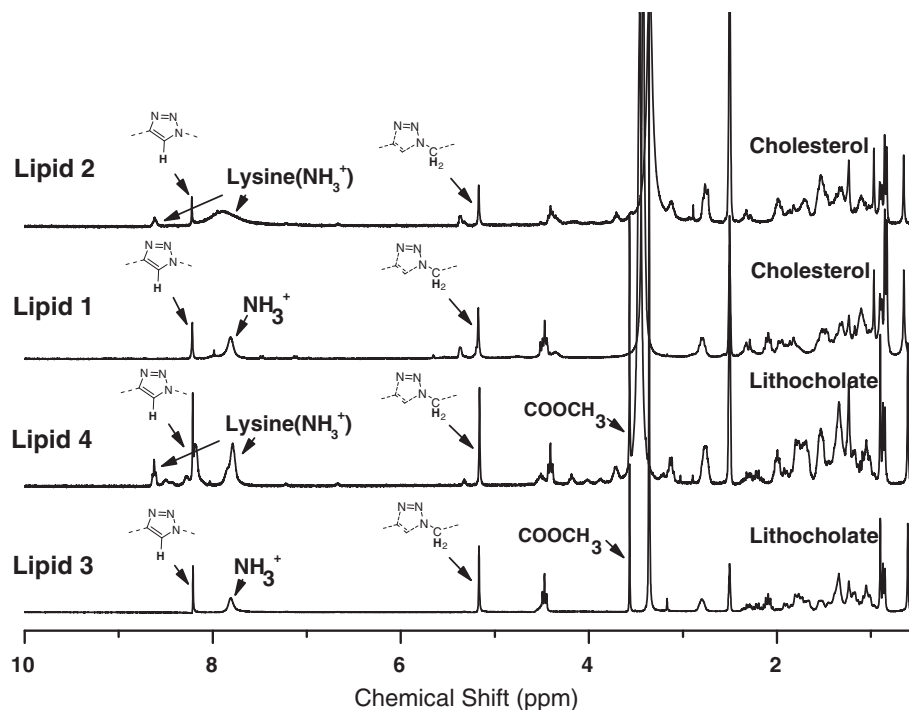


Figure 1. ^1H NMR spectra of Steroid-based cationic lipids **1–4** in $\text{DMSO-}d_6$ solution. The magnetic frequency was set as 300 MHz.

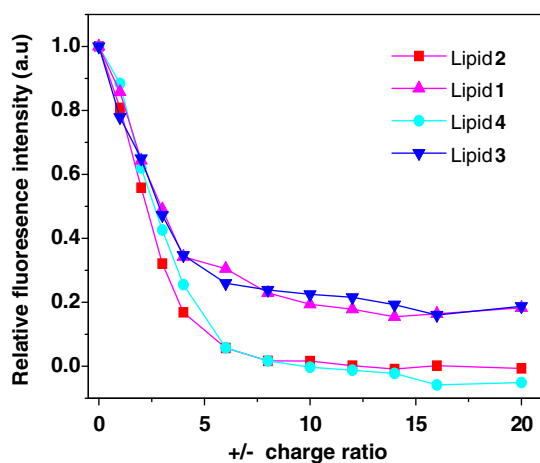


Figure 2. Ethidium bromide displacement assay of plasmid DNA binding affinities for the steroid-based cationic lipids **1–4** under various \pm charge ratios in 0.01 M PBS buffer solution.

completely at the \pm charge ratio of 2–4, while **1** and **3** showed lower pDNA binding affinity with a complete pDNA retardation at \pm charge ratio of 4–6, elicited the conduction of (*l*)-lysine (diamine) headgroup could enhance the pDNA binding affinity of the sterol-based cationic lipids, and which was consistent with the results of EB displacement assay. Similarly, we previously reported a series of disulfide-containing cholesterol lipids (CHOSS),³⁸ which also demonstrated complete pDNA retardation/binding at the N/P (\pm) ratio of 2–6. These results indicated that the newly synthesized sterol-based cationic lipids could achieve high pDNA binding/loading affinities.

2.3. Hydrodynamic particle size and zeta potential

It had been revealed that cell adhesion and intracellular uptake behaviors were greatly affected by morphology of aggregated

lipoplexes such as size and shape,⁴⁶ which strongly depended on the molecular structures including hydrophobic/philic blocks, chemical linkages, as well as headgroups.⁴⁷ Herein, the hydrodynamic particle size and zeta potential of the sterol-based cationic lipids/pDNA lipoplexes were measured by dynamic laser scattering instrument (DLS). As shown in Figure 4a, the average particle sizes of all lipoplexes could be seen increased from 220–320 nm to 390–570 nm at the \pm ratio range from 2 to 6, then the sizes decreased at the \pm charge ratio higher than 6, elicited the cationic lipids-induced pDNA condensation and the formation of the lipoplexes.⁴⁸ Among them, (*l*)-lysine headgroup bearing lipids (**2** and **4**) formed larger lipoplexes (480–570 nm) than that of monoamine headgroups bearing lipids (**1** and **3**, 250–420 nm lipoplexes), indicated the type of headgroup play vital roles in the formation of lipoplexes. Moreover, it could be noticed that there was no obvious particle size difference between **2**/pDNA and **4**/pDNA lipoplexes, whereas **3**/pDNA lipoplex showed an obviously smaller average particle size (250–390 nm) than that of **1**/pDNA (390–420 nm) within the \pm ratio range from 6 to 24, indicated the particle size of lipoplex aggregates did not only depends on the headgroups, but also on the skeleton structure of the sterol lipids. Moreover, it could be expected that the sterol-based cationic lipids/pDNA lipoplexes might have different uptake or intracellular behaviors due to their different hydrodynamic particle sizes. On the other hand, the surface charges of all sterol-based lipids/pDNA lipoplexes increased from -22 to -15 mV to $+22$ to $+36$ mV with the gradually increasing of the \pm charge ratio up to 20 (Fig. 4b). It could be found that the surface charge converted from negative to positive (Fig. 4b) at low \pm charge ratio of about 2–5, indicated the ‘Click’ synthesized sterol-based cationic lipids could efficiently bind with pDNA. In addition, the positive zeta potential of the lipoplexes was expected to facilitate their adhesion process onto negative-charged cell membrane.

2.4. Morphology study by AFM

The morphology of the sterol-based cationic lipids/pDNA lipoplexes were further investigated by atomic force microscopy

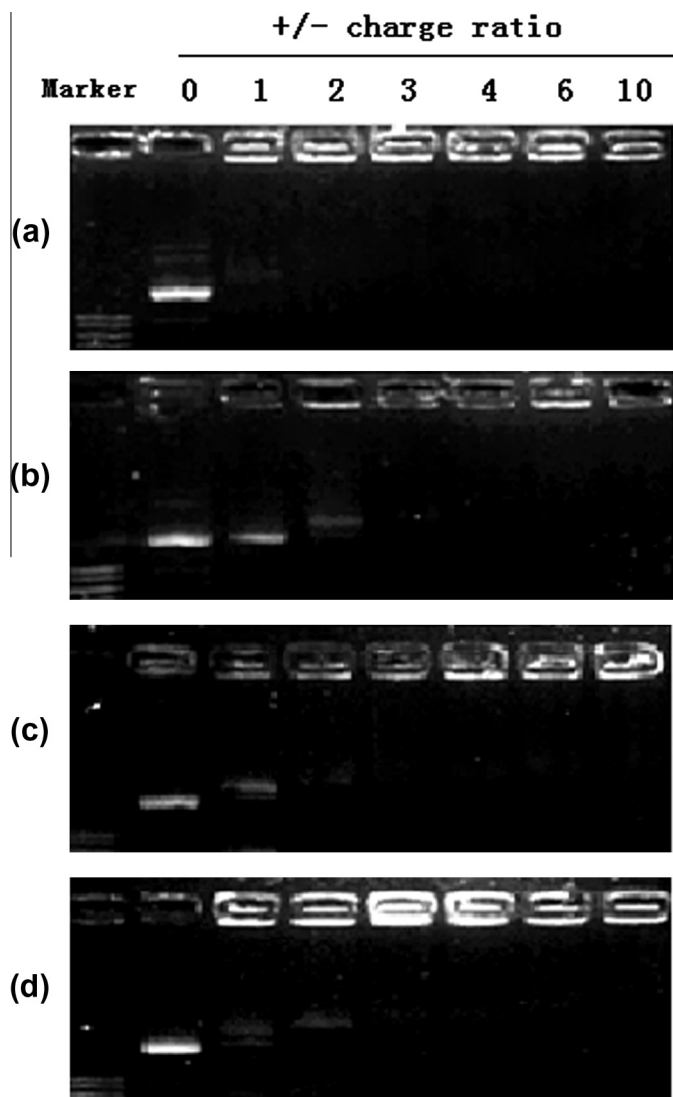


Figure 3. Agarose-gel retardant assay of pDNA binding affinity with the addition of the steroid-based cationic lipids (a) lipid 4, (b) lipid 3, (c) lipid 2, (d) lipid 1 at various +/- charge ratios.

(AFM), and all the lipoplexes were as-prepared at +/- ratio of 15. As shown in Figure 5, 1/pDNA, 2/pDNA and 4/pDNA lipoplexes are observed as near-spherical shaped³⁸ nanoparticles with average

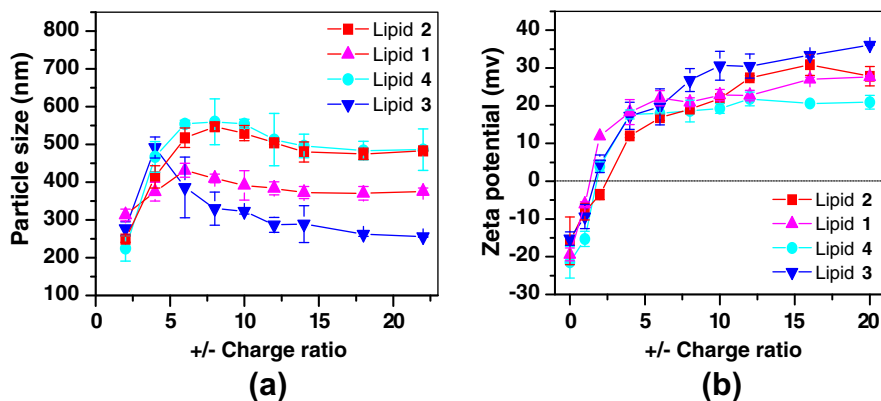


Figure 4. Average particle sizes (a) and zeta potentials (b) of the steroid-based cationic lipids 1–4/pDNA lipoplex aggregates under various +/- charge ratios were measured by dynamic light scattering analysis at room temperature with a laser wavelength $\lambda = 633$ nm and a scattering angle of 90° .

diameter of about 70–210 nm, however, 3/pDNA lipoplex demonstrated much smaller particle sizes around 30–70 nm, indicated that the particle size of the lipoplexes could be greatly influenced by the structure of the sterol-based lipids. It could also be noticed that the lipoplex sizes observed by AFM (70–210 nm) is much smaller than that measured by DLS (280–500 nm) at +/- ratio of 15, the difference between AFM and DLS results could be interpreted as the hydration effect of lipoplexes could result in the formation of larger 'swelled' particles in DLS measurement,⁴⁹ whereas the drying process of lipoplexes would produce smaller 'shranked' particles in AFM observation.⁵⁰ Moreover, since the accuracy of DLS measurement are greatly influenced by solution, particle shape and size distribution, alternatively, AFM was often employed as a more efficient method to directly observe and identify nanoparticles.⁵¹

2.5. Cytotoxicity of sterol-based cationic lipids by MTT assay

Cytotoxicity was regarded as an essential restriction element in practical application of gene carriers. To develop new synthetic gene carriers with the merit of low cytotoxicity and high transfection efficacy, the dependence of cytotoxicity on the molecular structure factors⁵² should be taken into account. As shown in Figure 6a and b, the in vitro apparent cytotoxicity of the sterol-based cationic lipids were examined in A549 and HeLa cells by MTT method, with bPEI-25k as the control. Lower cell cytotoxicities in both A549 and HeLa cells could be observed when incubated with lipid 4 ($IC_{50} = 63.8 \mu\text{g/mL}$ in A549; and $IC_{50} = 41.9 \mu\text{g/mL}$ in HeLa), and higher cytotoxicity ($IC_{50} = 19.6 \mu\text{g/mL}$ in A549; and $IC_{50} = 27.0 \mu\text{g/mL}$ in HeLa) was observed after incubation with lipid 2. Meanwhile, the lithocholate-bearing lipid 3 showed an drastically high cytotoxicity ($IC_{50} = 13.9 \mu\text{g/mL}$ in HeLa), which almost approached to the same level of the control bPEI-25k ($IC_{50} = 11.5 \mu\text{g/mL}$ in HeLa), and even higher cytotoxicity ($IC_{50} = 5.6 \mu\text{g/mL}$) than that of bPEI-25k ($IC_{50} = 13.8 \mu\text{g/mL}$) in A549 cells, whereas its cholesterol-bearing analog 1 showed much lower cytotoxicity ($IC_{50} = 73.6 \mu\text{g/mL}$ in A549; and $IC_{50} = 52.8 \mu\text{g/mL}$ in HeLa). These results demonstrated the structural elements including the sterol skeletons, linkers and headgroups strongly affected the apparent cytotoxicity. Besides, we found that lipid 2 showed moderate cytotoxicity ($IC_{50} = 124 \mu\text{g/mL}$ in COS-7), higher than that of our earlier synthesized (*l*)-lysine headgroup-bearing cholesterol disulfide lipid CHOSS-Lys ($IC_{50} = 241 \mu\text{g/mL}$ in COS-7),³⁸ elicited the triazole ring might play some roles in apparent cytotoxicity.

2.6. Cytotoxicity of sterol-based cationic lipids by LDH assay

Cell plasma membrane damage/destruction was regarded as one of the important elements that caused cytotoxicity. Herein,

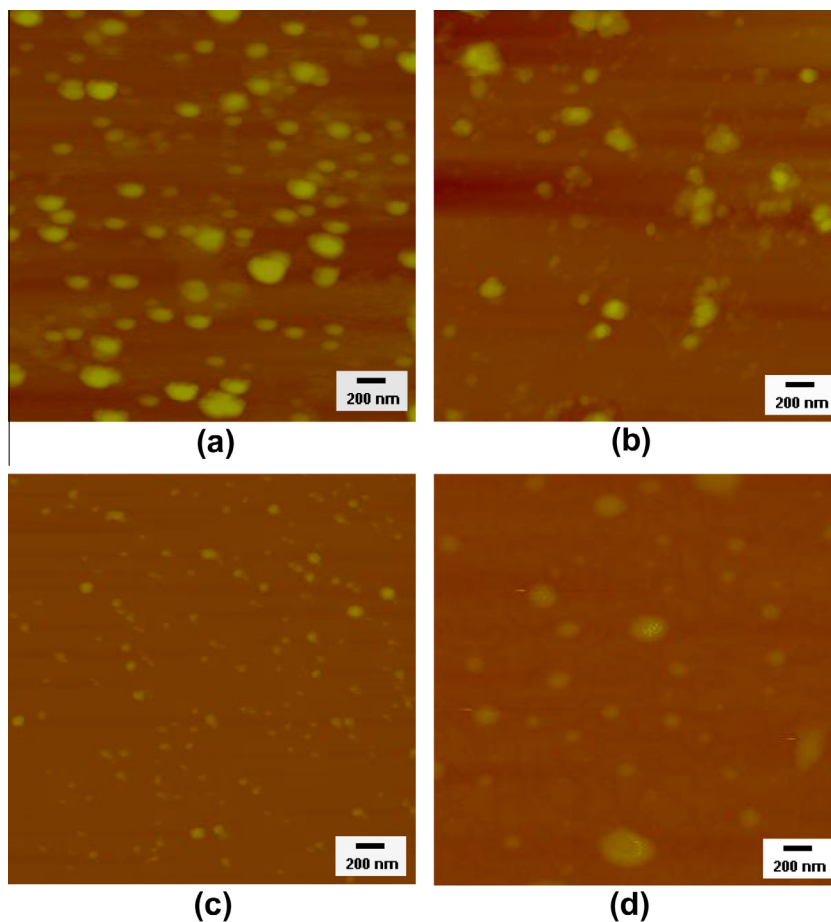


Figure 5. AFM morphologies of the steroid-based cationic lipids/pDNA lipoplex aggregates at the \pm charge ratio of 15 (a) lipid 1/pDNA, (b) lipid 2/pDNA, (c) lipid 3/pDNA, (d) lipid 4/pDNA. Each of the samples were scanned in the tapping mode.

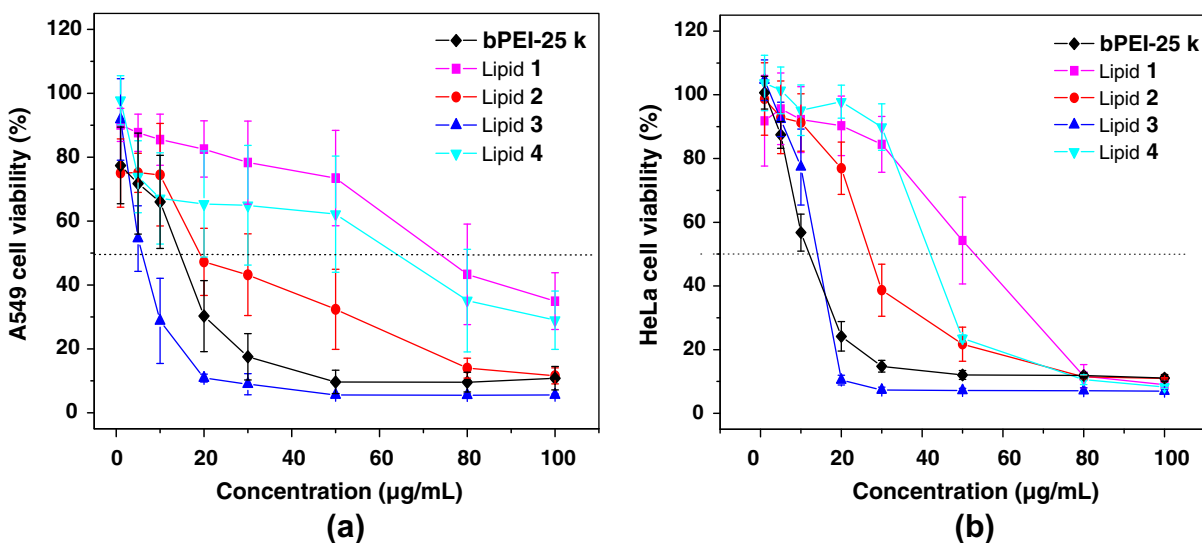


Figure 6. The cytotoxicity (MTT) assays of the steroid-based cationic lipids in various concentrations (from 0 to 200 µg/mL) (a) in A549 cells (b) in HeLa cells.

to further understand the mechanism of the cytotoxicity induced by the sterol-based cationic lipids, lactate dehydrogenase (LDH) assay was employed for quantitative evaluation of the plasma membrane damage mediated by lipids 1–4 under the equal concentration of 50 µg/mL in HeLa cells.⁵³ As shown in Figure 7, it could be noted that lipids 1, 2 and 4 showed slightly plasma

membrane damage effects (<3.0%), lower than that of the control lipofectamine 2000 (5.8%). Meanwhile, lipid 3 showed much higher plasma membrane damage (28.3%) in HeLa cells, which reached one third of that of bPEI-25k (83.1%). On the other hand, it could be noted that 3 showed higher apparent cytotoxicity than bPEI-25K in HeLa cells under the concentration of 50 µg/mL in MTT

assay (Fig. 6b), however, it showed much lower cytotoxicity (membrane damage) than that of bPEI-25k in LDH assay, suggested that the plasma membrane damage effect of lipid **3** might only partially contribute to its apparent cytotoxicity. Thus, we deduced that apart from cell membrane damage, the rest of the apparent cytotoxicity of **3** might be attributed to its metabolism-related intracellular processes such as the activating of pregnane X receptor (PXR, NR1I2) by the lithocholated metabolite 3-keto-LCA or other Xenobiotic ligands.⁵⁴ Moreover, to some extent, it could be seen that the trend of cytotoxicity of lipid **1–4** in LDH assay was consistent with that in MTT assay.

2.7. Luciferase transfection assay of sterol-based cationic lipids

The gene transfection efficiency of the sterol-based cationic lipids was evaluated by luciferase gene expression assay in A549, HeLa (Fig. 8), as well as HEK293T (Fig. S2) cell lines. The lipoplexes were firstly prepared by mixing the sterol-based cationic lipids with pDNA at various +/- charge ratios. It could be seen that the relative luciferase gene expression level of these sterol-based cationic lipids was quite different in all of the cell lines. Lipid **2**, which bearing both cholesterol skeleton and (*l*)-lysine headgroup, showed the highest optimum luciferase gene transfection capability (6.1×10^4 RLU/mg protein in A549 and 6.6×10^5 RLU/mg protein in HeLa cells) at the +/- charge ratio of 5, which reached 1.3–4.0-fold higher transfection efficacy of bPEI-25k (1.5×10^4 RLU/mg protein in A549 and 5.0×10^5 RLU/mg protein in HeLa) and 0.15–0.25-fold of lipofectamine2000 (2.7×10^5 RLU/mg in A549 and 4.9×10^6 RLU/mg protein in HeLa). When transfected with lipid **1**, much lower luciferase expression (5.6×10^2 RLU/mg protein in A549 and 2.3×10^4 RLU/mg protein in HeLa) was observed. The higher transfection efficacy of lipid **2** compared to **1** might be attributed to the enhanced cellular uptake and 'endosomal escape' effect mediated by the (*l*)-lysine headgroup attached to lipid **2**.^{38,55} However, the lithocholate-bearing lipids **4** and **3** do not show such obvious gene transfection capacity in A549, HeLa (Fig. 8) and HEK293T (Fig. S2) cells, in contrast, they demonstrated very low transfection efficiency in A549 and HeLa, and even negligible efficiency in HEK293T cells. Similar results could also be seen in pEGFP gene transfection (Fig. S3). It could be noted that the lipid **2** and **4**, both bearing a (*l*)-lysine headgroup, possessed quite different gene delivery capacity, despite their similar pDNA binding affinity, lipoplex particle size and zeta potential. Besides, Lipid **3** showed much lower transfection efficacy than **1**, although its lipoplex size was

smaller. The results suggested that not only cationic headgroups, but also sterol skeletons of the sterol-based cationic lipids, played vital roles in gene transfection. Moreover, among the cationic lipids, lipid **2** achieved the highest gene transfection efficiency, while its efficiency is not optimized to the maximum level yet. Thus, for practical application, it is necessary to optimize lipid **2** by developing its new formulations (e.g., lipid **2**-based liposomes) in the future. In addition, we further calculated and estimated the rough material cost for lipid **2** (about \$17.2/mg), which seems much lower than that of commercially available lipofectamine2000 (Invitrogen, USA, about \$204.2/mg), indicated lipid **2** could be developed as a potential transfection reagent for high efficient gene delivery.

It had been known that gene transfection strongly relied on two consecutive processes: the intracellular uptake, and the intracellular trafficking/localization of lipoplexes. Herein, we investigated the cellular uptake of the sterol lipids/Cy3-pDNA lipoplexes (Fig. S4) by fluorescence microscopy, and pDNA was pre-labeled with a red-fluorescent agent Cy3 by a Label IT[®] Tracker[™] Cy3-labeling kits.³⁸ It could be observed that the red fluorescence were dispersed in the cells after 4 h incubation of the sterol lipids/Cy3-pDNA lipoplexes, similar to that of lipofectamine2000/Cy3-pDNA polyplexes, while only weak red fluorescence could be seen in the cell incubated with naked Cy3-pDNA, indicated the Cy3-pDNA could be efficiently transferred into the cells by using sterol-based cationic lipids as the carriers. Although the intracellular uptake of pDNA mediated by sterol lipids have been successfully observed, however, the structural dependence of the uptake pathway of these sterol-based cationic lipids was still not known. Recently, Doh and co-workers⁵⁶ revealed that a cholesterol-derived cationic lipid Chol-E mainly underwent a clathrin-dependent uptake pathway and showed membrane cholesterol depletion resistance. In this case, we supposed that the cholesterol and lithocholate based lipids might pass through different structure-dependent endocytosis pathways to enter the cell, since different intracellular uptake pathway (such as clathrin, caveolae, lipid-raft, phagocytosis, pinocytosis mediated endocytosis, and so on) of the carriers/pDNA complexes might lead to different results of gene transfection. The related study on the endocytosis pathways of the sterol cationic lipids by using of the specific pathway inhibitors was carrying out in our current research.

2.8. Intracellular trafficking/localization of the sterol-based cationic lipids

It had been revealed that intracellular trafficking/localization of lipoplexes might influence the gene delivery efficacy. The intracellular localization of the sterol-based cationic lipids/ Cy3-labeled pDNA lipoplexes in HeLa cells were studied by fluorescence microscope with bPEI-25K as a control, and the cell nuclei and lysosome were separately labeled with fluorescent dyes DAPI (blue) and LysoTracker (green), respectively. As shown in Figure 9, after 4 h transfection with 1/Cy3-pDNA lipoplex, it could be clearly seen that red fluorescent spots dispersed inside cell plasma, and some of them located around or within the DAPI-stained nucleus, but few of them was found in lysosome. In contrast, after incubation with 3/Cy3-pDNA lipoplex, some red fluorescent spots were observed located on the outside of plasma membrane, which might be related to the membrane destruction effect of **3**. Meanwhile, when incubated with 2/Cy3-pDNA and 4/Cy3-pDNA lipoplexes, red fluorescence spots were observed uniformly distributed inside the plasma membrane and co-localized with the lysosome, the lysosomal co-localization behavior might be attributed to the proton buffering effect of the (*l*)-lysine headgroups. Likewise, the bPEI-25k/pDNA polyplex also presented an obvious lysosomal co-localization behavior, due to its well-known 'proton sponge' effect. The results demonstrated that the intracellular localization of the

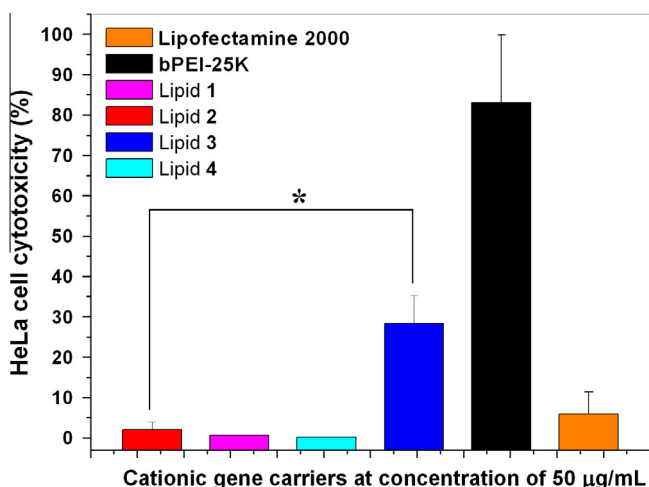


Figure 7. LDH cytotoxicity assays of the steroid-based cationic lipids (50 µg/mL) in HeLa cells. (**p* < 0.05%).

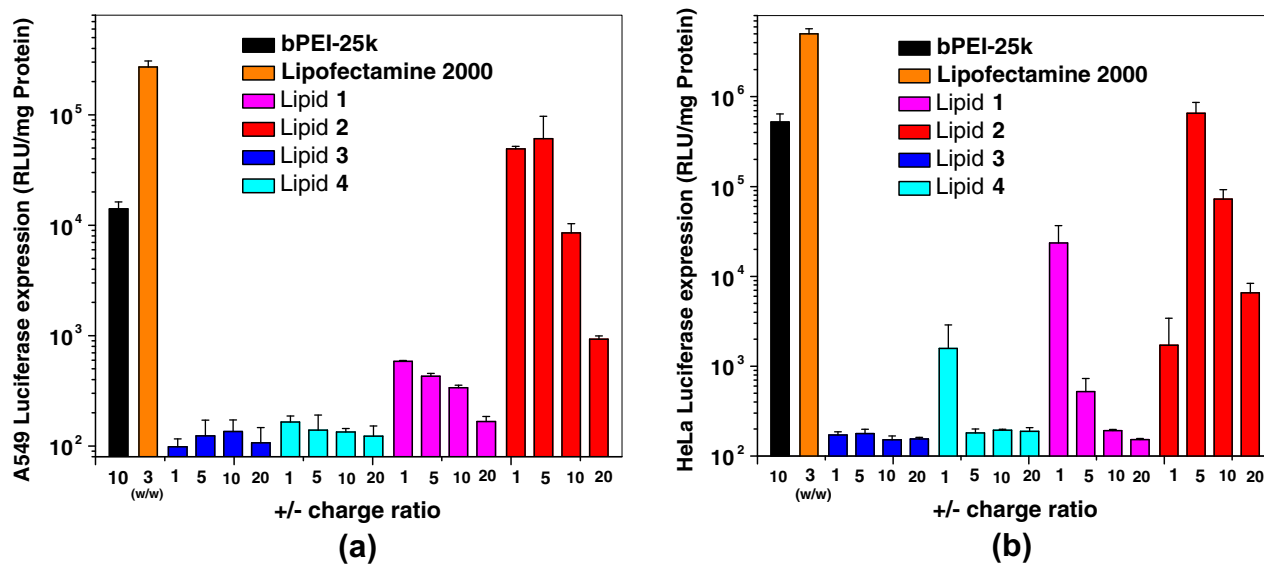


Figure 8. Luciferase gene transfection efficiencies for the steroid-based cationic lipids/pDNA complexes under various +/- charge ratios in (a) A549 and (b) HeLa cell lines, and commercially available bPEI-25k and lipofectamine 2000 was used as controls.

enveloped Cy3-pDNA could be affected by the molecular structure (including sterol skeletons and headgroups) of the sterol-based cationic lipids. Moreover, it could be interestingly noticed that lipid 2 and 4 have similar intracellular localization effect but quite different gene transfection efficiencies, elicited some unknown mechanisms/factors might regulate the gene transfection efficacy. Furthermore, the endocytosis pathways and intracellular trafficking mechanisms of the sterol-based cationic lipids were under investigation in our lab.

3. Conclusion

In summary, we successfully prepared a series of new sterol-based cationic lipids by modularly and efficiently incorporate sterol-based hydrophobic blocks with cationic building blocks via 'Click' chemistry approach. It was found that these synthesized cationic lipids could bind/load pDNA efficiently. The physico-chemical properties of their pDNA lipoplexes, such as particle sizes, morphologies and surface charges were found greatly depend on the molecular structure factors including sterol skeletons and headgroups. On the other hand, these sterol-based cationic lipids were found exhibit quite different cytotoxicity and luciferase gene transfection efficacy, which also strongly-relied on their molecular structures. Interestingly, the cholesterol-bearing lipids **1** and **2** showed much higher transfection capability (7–10⁴ times) than their lithocholate-bearing counterparts **3** and **4**, suggested that cholesterol could be employed as an more efficient moiety than lithocholate for constructing new lipid gene carriers. Among the lipids, it could be noted that lipid **2** achieved high gene transfection capability, made it an efficient transfection agent candidate for efficient gene delivery application. Finally, the study also provided an efficient and promising approach for developing low cytotoxic and high efficient lipid gene carriers by selecting suitable sterol hydrophobes and cationic headgroups as the building blocks.

4. Experimental section

4.1. Materials

Cholesteryl chloroformate (**12**, 97%) was purchased from Acros Organics and utilized as received. Methyl lithocholate-3-hydroxy

chloroformate (**13**) was prepared according to literature.⁵⁷ Propargyl alcohol (97%) was supplied by Alfa Aesar and used as received. 3-Bromo-1-propamine (**11**, 99%) was bought from Aladdin, Shanghai. N-(3-dimethyl-aminopropyl)-N'-ethylcarbodiimide hydrochloride (EDC-HCl, 99%), 4-dimethyl amino pyridine (DMAP) and trifluoroacetic acid (TFA) were provided by Shanghai Sinopharm Chemical Reagent Co. Ltd, CuSO₄·5H₂O (99%) and sodium ascorbate (98%) were purchased from Shanghai Sinopharm Chemical Reagent Co. Ltd and utilized as-received. Boc-(L)-lysine was synthesized as refer to the published literatures.⁵⁸ Other reagents and solvents were analytical grade and utilized as received.

Agarose was purchased from Gene Tech, Shanghai. Ethidium bromide (EB) (95%) and branched poly(ethylene imine) (bPEI-25k, M_w = 25,000) were supplied by Sigma & Aldrich. Lipofectamine™2000 was received from Invitrogen (USA) (lot no. 637822). Thiazoyl blue tetrazolium bromide (MTT) was bought from Biobasic Inc, (Markham, Canada), lactate dehydrogenase (LDH) cytotoxicity assay kit II (Cat#ab65393) were provided by Abcam Corporation (UK). Luciferase assay and bicinchoninic acid (BCA) protein quantization kits were supplied by Promega (USA) and Appligen Technologies (Beijing, China), respectively. 0.01 M phosphate buffer solution (1× PBS), DMEM medium and 10% fetal bovine serum (FBS) were purchased from Hangzhou Genom Co. Ltd. 96-well and 24-well microplates and 50 mL cultivation flasks were received from Corning Co. Ltd. Human epithelial cervical cancer (HeLa), Human Embryonic Kidney (HEK293-T), Carcinomic human alveolar basal epithelial (A549) cell lines were provided by Dr. Bo Wan of state key laboratory of genetic engineering of Fudan University, Shanghai, and African Green Monkey Kidney (COS-7) cell line was generously provided by the laboratory of Prof. Yuhong Xu (School of Pharmacy, Shanghai Jiaotong University). Luciferase gene (pCMV-Luc) and pEGFP plasmid DNA were prepared and purified in our own laboratory. Label IT® Tracker™ intracellular nucleic acid (Cy3-labeled pDNA) localization kits including Trans IT®-LT1 transfection reagent was purchased from Mirus Bio LLC, USA. Lysotracker green DND-26 was received from Invitrogen (Cat#L7526, USA). DAPI was received from Roche (Cat#70217321, USA). In addition, all the other reagents and chemicals were of analytical grade, and were utilized as-received.

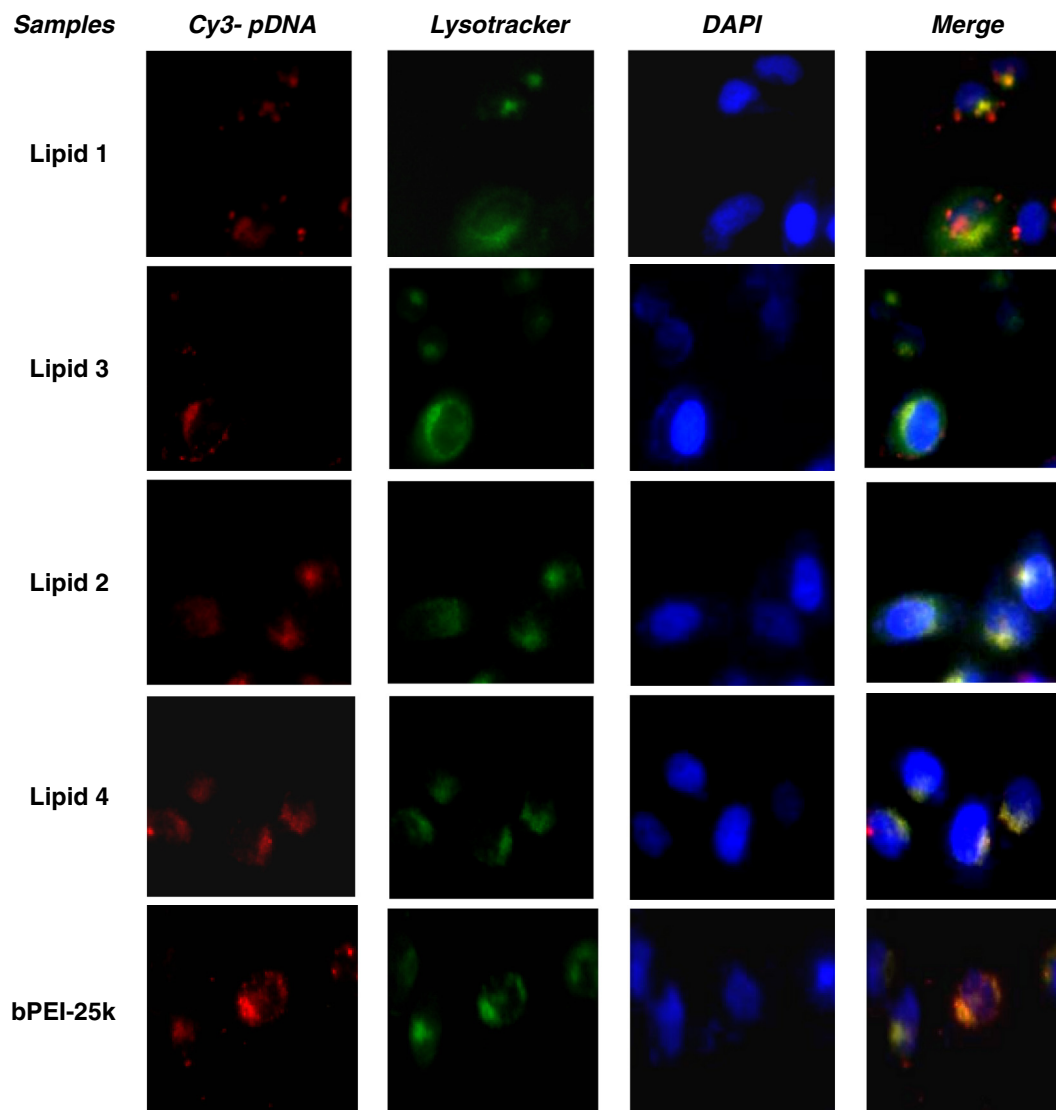


Figure 9. Fluorescence images (400 \times) of intracellular trafficking of the Cy3-labeled pDNA enveloped by the steroid-based cationic lipid gene carriers (lipid 1–4) for 4 h in HeLa cells, bPEI-25K was use as reference. (Red: cy3-labeled pDNA; green: Lysotracker stained endosome/lysosome; blue: DAPI stained cell nuclei).

4.2. Preparation procedures of sterol-based cationic lipids

4.2.1. Synthesis of sterol-propynyl building blocks

4.2.1.1. Synthesis of cholesteryl-3-hydroxy-2-propynyl carbamate (5). Cholesteryl chloroformate (**12**, 7.4 g, 0.02 mol) dissolved in 50 mL of dichloromethane was added dropwise into a 100 mL flask with propargyl alcohol (5.6 g, 0.1 mol) and 10 mL pyridine dissolved in 20 mL of dichloromethane. The mixture was kept stirring for 12 h at room temperature, and then poured into 100 mL of distilled water and further extracted with 150 mL ethyl acetate (EtOAc). The aqueous phase was discarded, and the organic phase was collected and concentrated under reduced pressure, and continuously purified by flash column chromatography (eluent: EtOAc/hexane = 1/2, v/v) to get cholesteryl-3-hydroxy-2-propynyl carbamate (**5**) as white solid (8.2 g, 92.7% yield).

$^1\text{H NMR}$ (CDCl_3 , 300 Hz) δ 5.40 (s, 1H, CH=C, cholesterol), 4.72 (s, 2H, C \equiv CCH $_2$), 4.57 (m, 1H, -CH-), 2.52 (s, 1H, C \equiv CH), 2.23–0.61 (m, 45H, cholesterol).

4.2.1.2. Synthesis of methyl lithocholate-3-hydroxy-2-propynyl carbamate (6). Methyl lithocholate-3-hydroxy chloroformate (**13**, 7.8 g, 0.02 mol) dissolved in 50 mL of dichloromethane was

added dropwise into a 100 mL flask with propargyl alcohol (5.6 g, 0.1 mol) and 10 mL pyridine dissolved in 20 mL of dichloromethane. The mixture was kept stirring for 12 h at room temperature, and then poured into 100 mL of distilled water and further extracted with 150 mL EtOAc. The aqueous phase was discarded, and the organic phase was collected and concentrated under reduced pressure, and continuously purified by flash column chromatography (eluent: EtOAc/hexane = 1/2, v/v) to get methyl lithocholate-3-hydroxy-2-propynyl carbamate (**6**) as white solid (6.7 g, 75.2% yield).

$^1\text{H NMR}$ (CDCl_3 , 300 Hz) δ 4.72 (s, 2H, C \equiv CCH $_2$), 4.57 (m, 1H, -CH-), 3.66 (s, 3H, COOCH $_3$), 2.52 (s, 1H, C \equiv CH), 2.21–0.61 (m, 38H, lithocholate).

4.2.2. Preparation of azido-bearing cationic blocks

4.2.2.1. Synthesis of 3-Bromo-1-propamine-NHBOC (9). In a 100 mL flask with 3-Bromo-1-propamine hydrobromide salt (**11**, 4.4 g, 0.02 mol) and pyridine (10 mL) dissolved in 100 mL tetrahydrofuran/20%NaOH (w/w) aqueous solution (v/v = 1/1) mixed solution, then di-*tert*-butyl dicarbonate (Boc $_2$ O, 4.8 g, 0.022 mol) dissolved in 20 mL tetrahydrofuran was added dropwise and the mixture was kept stirring for 6 h under room temperature. After

that, the reaction mixture was poured into distilled water and extracted with EtOAc, dried with MgSO₄ anhydride and concentrated under reduced pressure, and the crude product was purified by flash column chromatography (eluent: EtOAc/hexane = 1/4, v/v) to obtain 3-Bromo-1-propamine-NHBOC (**9**) as a yellowish oil (3.1 g, 62.6% yield).

¹H NMR (CDCl₃, 300 Hz) δ 4.31(1H, -CHCON-), 3.34(2H, -CH₂-), 3.11(2H, -CH₂-), 1.99(2H, -CH₂-), 1.27 (9H, Boc).

4.2.2.2. Synthesis of 3-azido-1-propamine-NHBOC (7). In a 100 mL flask with 3-Bromo-1-propamine-NHBOC (**9**, 2.3 g, 0.01 mol) and sodium azide (0.72 g, 0.011 mol) dissolved in 5 mL DMF the mixture was kept stirring for 8 h at 80 °C. Then the mixture was cooled down and gently poured into 100 mL distilled water, then extracted with 100 mL EtOAc, the solvent phase was concentrated under reduced pressure, and crude 3-azido-1-propamine-NHBOC (**7**) was obtained and utilized directly without further purification.

4.2.2.3. Synthesis of 3-Bromo-1-propamine-NH-lysine-BOC (10). In a 100 mL flask with 3-Bromo-1-propamine hydrochloride salt (**11**, 2.2 g, 0.01 mmol) and Boc-(*L*)-lysine (3.5 g, 0.01 mol) were dissolved in 20 mL tetrahydrofuran with 10 mL pyridine, then EDC·HCl/DMAP (3.0 g/0.1 g) was added and the mixture was kept stirring for 24 h under the room temperature. After that, the mixture was gently poured into 100 mL distilled water and extracted with 100 mL EtOAc, the organic solvent phase was washed with distilled water and concentrated under reduced pressure, and purified by flash column chromatography (eluent: EtOAc/hexane = 1/3, v/v) to get 3-Bromo-1-propamine-NH-lysine-BOC (**10**) as a colorless oil (2.6 g, 56.5% yield).

¹H NMR (CDCl₃, 300 Hz) δ 4.28(1H, -CHCON), 3.42(2H, -CH₂-), 3.11(2H, -CH₂-), 2.05 (2H, -CH₂-), 1.42 (18H, Boc).

4.2.2.4. Synthesis of 3-azido-1-propamine-NH-lysine-BOC (8). In a 100 mL flask with 3-Bromo-1-propamine-NH-lysine-BOC (**10**, 1.2 g, 0.0025 mol) and sodium azide (0.33 g, 0.005 mol) dissolved in 10 mL DMF and was kept stirring for 8 h under 80 °C. Then the mixture was cooled down and gently poured into 50 mL distilled water, then extracted with 100 mL EtOAc, the solvent phase was concentrated under reduced pressure, and crude 3-azido-1-propamine-NH-lysine-BOC (**8**) was obtained and utilized directly without further purification.

4.2.3. General procedures for the synthesis of sterol-based cationic lipids (1–4) by CuAAC 'Click' method

In a 100 mL flask added with as-prepared sterol-propynyl building blocks (**5** or **6**, 1.0 mmol) and azido-bearing cationic blocks (**7** or **8**, 1.1 mmol) in 20 mL tetrahydrofuran, and quickly added CuSO₄·5H₂O/Sodium ascorbate (0.5 mmol/1 mmol) which were firstly dissolved in 5 mL distilled water, the reaction mixture was kept at 80 °C for 2 h, the yellow solid was removed by filtration and the filtrate was added with 50 mL 5% EDTA (w/w) aqueous solution to coordinate excessive Cu(I), then extracted with 100 mL EtOAc. After that, the solvent was removed under reduced pressure, then the yellow residue was purified by flash column chromatography (EtOAc/Hexane = 1:1) to get Boc-protected sterol-based cationic lipids, which was reacted with excessive trifluoroacetic acid (5 mL) at room temperature for 1 h to remove the Boc protecting group, then the solvent trifluoroacetic acid was evaporated, the residue was precipitated with diethyl ether (Et₂O) and dried to get pure sterol-based cationic lipids **1–4** as the final products.

Lipid **1** (Yield:79%).

¹H NMR: (CDCl₃, 300 Hz) δ 8.17 (s, 1H, ArH, triazole), 7.89 (b, NH₃⁺), 5.32 (s, 1H, -C=CH-, cholesterol), 5.13 (s, 2H,

triazole-CH₂-OOC-), 4.44 (t, 2H, C-CH₂-triazole), 4.31 (m, 1H, -OOC-O-CH-), 2.77 (t, 2H, NH₃⁺-CH₂-), 2.47 (t, 2H, NH₃⁺-CH₂-CH₂-), 2.26–0.61 (45H, cholesterol).

¹³C NMR: (CDCl₃, 300 Hz) δ 154.1, 138.5, 124.8, 121.9, 76.5, 59.7, 55.4, 55.2, 54.8, 53.9, 48.7, 45.8, 41.1, 38.9, 38.8, 36.8, 35.5, 34.8, 34.3, 30.5, 26.9, 26.5, 22.9, 22.4, 21.7, 21.6, 19.8, 18.0, 17.5, 11.0

ESI-MS [M+H⁺]: 569.4, Calculated: 569.5.

Lipid **2** (Yield:69%).

¹H NMR: (CDCl₃, 300 Hz) δ 8.65 (b, NH₃⁺), 8.21 (s, 1H, ArH, triazole), 7.87 (b, NH₃⁺), 5.36 (s, 1H, -C=CH-, cholesterol), 5.16 (s, 2H, triazole-CH₂-OOC-), 4.51(s, 1H, -CH-CONH-), 4.40 (t, 2H, C-CH₂-triazole), 4.33 (m, 1H, -OOC-O-CH-), 3.11(t, 2H, -CONH-CH₂-), 2.77 (t, 2H, NH₃⁺-CH₂-), 2.47 (t, 2H, NH₃⁺-CH₂-CH₂-), 2.26–0.62 (45H, cholesterol).

¹³C NMR: (CDCl₃, 300 Hz) δ 169.1, 154.1, 139.6, 125.5, 122.8, 77.7, 60.7, 56.5, 55.9, 52.5, 49.8, 47.4, 42.3, 38.9, 38.8, 37.9, 36.7, 36.4, 36.2, 35.6, 31.7, 30.8, 29.9, 28.2, 27.7, 27.6, 27.0, 26.8, 24.1, 23.5, 23.1, 22.8, 21.6, 21.0, 19.1, 18.5, 12.1.

ESI-MS [M+H⁺]: 697.5; Calculated: 697.5.

Lipid **3** (Yield:62%).

¹H NMR: (CDCl₃, 300 Hz) δ 8.20 (s, 1H, ArH, triazole), 7.89 (b, NH₃⁺), 5.16 (s, 2H, triazole-CH₂-OOC-), 4.48 (m, 1H, -OOC-O-CH-), 4.47 (t, 2H, C-CH₂-triazole), 3.56 (s, 3H, -COOCH₃), 2.77 (t, 2H, NH₃⁺-CH₂-), 2.47 (t, 2H, NH₃⁺-CH₂-CH₂-), 2.26–0.61 (39H, lithocholate).

¹³C NMR: (CDCl₃, 300 Hz) δ 174.3, 154.3, 142.0, 125.6, 123.9, 78.3, 60.5, 56.2, 55.9, 52.8, 51.7, 48.3, 47.0, 42.6, 41.5, 38.8, 36.7, 35.7, 35.2, 34.6, 33.1, 32.1, 30.7, 27.3, 27.0, 26.3, 24.2, 23.3, 21.6, 20.6, 18.4, 12.1.

ESI-MS [M+H⁺]: 573.3; Calculated: 573.5.

Lipid **4** (Yield: 66%).

¹H NMR: (CDCl₃, 300 Hz) δ 8.67 (b, NH₃⁺), 8.20 (s, 1H, ArH, triazole), 7.89 (b, NH₃⁺), 5.15 (s, 2H, triazole-CH₂-OOC-), 4.48 (m, 1H, -OOC-O-CH-), 4.47 (t, 2H, C-CH₂-triazole), 4.17 (m, 1H, -NH₃⁺-CH-CONH-), 3.56 (s, 3H, -COOCH₃), 2.76 (t, 2H, NH₃⁺-CH₂-), 2.50(t, 2H, NH₃⁺-CH₂-CH₂-), 2.26–0.61 (39H, lithocholate).

¹³C NMR: (CDCl₃, 300 Hz) δ 174.3, 169.0, 154.3, 141.7, 125.4, 123.9, 78.1, 60.4, 56.3, 55.8, 52.6, 52.0, 51.3, 47.5, 42.8, 41.5, 40.4, 38.8, 36.3, 35.6, 35.1, 34.8, 34.6, 32.1, 31.0, 30.9, 29.9, 29.7, 28.0, 26.8, 26.5, 26.2, 24.0, 23.3, 21.6, 20.6, 18.3, 12.0.

ESI-MS [M+H⁺]: 701.5; Calculated: 701.5.

4.3. NMR and mass spectral measurements

¹H NMR spectra were characterized under room temperature on a Varian VXR-300 Fourier transform NMR spectrometer at 300.0 MHz for proton nuclei, and ¹³C NMR spectra were measured on a Bruker Avance NMR spectrometer at 100.0 MHz for the ¹³C nuclei, and tetramethylsilane (TMS) was utilized as the internal chemical shift reference. Mass spectra (ESI-MS) were routinely measured on a Varian SATURN 2000 instrument.

4.4. Ethidium bromide replacement assay

Ethidium bromide (0.5 μg) and pDNA (Luciferase pDNA, 4.0 μg) were firstly mixed in 1 mL of 0.01 M PBS buffer solution (pH 7.4), and kept incubation at room temperature for 2 min. Then, each sterol-based cationic lipids under various +/- charge ratios of 0.5–20 was separately placed into the pDNA/EB mixture solution, and continuously kept incubation for 10 min. Subsequently, fluorescence spectra for the above complex solution were recorded on a Hitachi F-7000 fluorescence spectrometer with excitation and emission wavelength at λ = 510 and 590 nm, respectively, and the emission intensities of the initial pDNA/EB mixture solution (*I*₁₀₀) and a pDNA-free EB solution (*I*₀) were taken as the corresponding

references of relative intensity 100% (F_{100}) and 0% (F_0). Furthermore, the emission intensities at 590 nm (I) for the pDNA/EB mixture solution under various $+/-$ charge ratios were measured, and their relative intensities F were calculated in accordance to $F = (I - I_0)/(I_{100} - I_0)$.

4.5. Agarose gel retardation assay

The pDNA binding capacities of the new sterol-based cationic lipids was investigated by agarose gel retardation assay. The solution of sterol-based cationic lipids/pDNA lipoplex was first prepared under a predetermined $+/-$ charge ratio with 0.01 M PBS and 1.0 μg of pDNA in 20 μL of pure water and kept incubation for 30 min. Then, the lipoplex solution was loaded onto 1% agarose gel (w/v) with EB (0.5 $\mu\text{g}/\text{mL}$ in gel) and TAE buffer (pH 7.4), and the naked pDNA was used as the control. After the gel electrophoresis under +100 V for 1 h, the retardant of pDNA was recorded on a UVP benchtop 2UV transilluminator system.

4.6. Average particle sizes and zeta potentials of the lipids/pDNA lipoplexes

Average particle sizes and zeta potentials of the Sterol-based cationic lipids/pDNA lipoplexes were analyzed on a Malvern Zetasizer Nano ZS90 (UK) at room temperature. The lipoplexes solution were first prepared by mixing sterol-based cationic lipids and pDNA (2.0 $\mu\text{g}/\text{mL}$) under diverse $+/-$ charge ratios in 1 mL of pure water, and then laser light at $\lambda = 633$ nm was employed at a fixed scattering angle of 90° for the nanoparticle size analyses.

4.7. Nanoparticle morphologies by atomic force microscopy

Nanoparticle morphologies of the sterol-based cationic lipids/pDNA lipoplexes were characterized at room temperature on a Nanoscope IVa atomic force microscopy (AFM, Veeco Instrument) in a tapping mode, and AFM measurements were conducted with Olympus AC160TS cantilever (Frequency: 300 kHz, stiffness: 42 N/m). The lipoplexes solution were first prepared by mixing sterol-based cationic lipids and pDNA (5.0 $\mu\text{g}/\text{mL}$) under the $+/-$ charge ratios of 15 in 1 mL of pure water, then the samples for AFM analysis were preliminarily prepared by dropping the as-prepared lipoplex solution onto fresh mica, and were air-dried at room temperature prior to AFM measurements.

4.8. MTT cytotoxicity assay of sterol-based cationic lipids

MTT assays were conducted with A549 and HeLa cell lines for evaluating cytotoxicities of synthesized sterol-based cationic lipids as well as their pDNA lipoplexes. Herein, the water-soluble sterol-based cationic lipids were dissolved into distilled water to prepare the stock solution (2 mg/mL for each cationic lipid). Firstly, the cells were seeded into 96-well microplates under 5×10^3 cells per well, and were cultivated under 37 °C and 5% CO_2 for 24 h in the 100 μL DMEM medium containing 10% FBS. Subsequently, the medium was replaced with fresh DMEM medium containing 10% FBS, and then the stock solution of sterol-based cationic lipids in predetermined amounts were added individually into the wells (with the final concentration ranging from 1 to 100 $\mu\text{g}/\text{mL}$) and commercially available branched-polyethylenimine (bPEI-25K) was utilized as a reference. After 24 h incubation, 20 μL of MTT (5.0 mg/mL) was added into each well, and kept incubation for 4 h. After removing the medium, DMSO (100 $\mu\text{L}/\text{well}$) was added to dissolve the formed MTT formazan. Finally, with gently shaking the microplates for 10 min for dissolving formazan, each sample with six replicates ($n = 6$) was analyzed on a microplate reader (BioTek, ELX800, USA) at $\lambda = 490$ ($\lambda = 630$ nm as reference

wavelength). In this study, a branched-polyethylenimine (bPEI-25k) was applied as a reference for MTT cytotoxicity assay.

4.9. LDH cytotoxicity assay of sterol-based cationic lipids

HeLa cells were seeded into 24-well microplates under 4×10^3 cells per well, and were cultivated under 37 °C and 5% CO_2 for 24 h in the 100 μL DMEM medium containing 10% FBS. Then each well was added with the stock solution of sterol-based cationic lipids (final concentration: 50 $\mu\text{g}/\text{mL}$), and commercially available branched-polyethylenimine (bPEI-25K) and lipofectamine 2000 were utilized as references. After that, 100 μL LDH reaction buffer was added into each well and the mixture was further incubated at room temperature for 30 min, the cells were centrifuged at 600 rpm for 10 min to precipitate the cells and its fragments. The clear supernatant (10 $\mu\text{L}/\text{well}$) was transferred into an optically clear 96-well plate. The samples were assayed with microplate reader (BioTek, ELX800, USA) at 490/630 nm as measure/reference wave length respectively. The results are calculated according to the protocol of LDH-Cytotoxicity Assay Kit II.

4.10. Luciferase transfection assay

For the Luciferase assay, A549, HeLa and HEK293T cells were firstly seeded into 24-well microplates (3×10^5 cells/well), and were incubated under 37 °C and 5% CO_2 with DMEM medium containing 10% FBS for 24 h. Lipoplexes solution were preliminarily prepared by mixing sterol-based cationic lipids (dissolved in 0.01 M PBS) and Luciferase pDNA (1.0 $\mu\text{g}/\text{well}$, dissolved in 0.01 M PBS) under a predetermined $+/-$ charge ratio. After 30 min standing, the prepared lipoplex solution was gently poured into the wells in the 24-well plates, and continued to incubate for 4 h with 200 μL FBS-free DMEM medium, and commercially available branched-polyethylenimine (bPEI-25K) and lipofectamine 2000 were utilized as references. Then the medium was replaced with 200 μL fresh DMEM medium containing 10% FBS and further incubated for 24 h. Consequently, the Luciferase transfection assays were conducted in accordance to the protocol of Promega Luciferase assay system. Finally, total luciferase protein was measured with BCA assay kit (Applygen Technologies Inc.), and relative light unit per milligram of Luciferase protein (RLU/mg) was thus calculated to evaluate the cell transfection efficacy of the sterol-based cationic lipids ($n = 3$).

4.11. pEGFP gene transfection assay

HeLa cells were seeded in 24-well plates at a density of about 5.0×10^4 cells/well with 200 μL DMEM medium (10% FBS, 37 °C, 5% CO_2). Lipoplexes solution were preliminarily prepared by mixing sterol-based cationic lipids (dissolved in 0.01 M PBS) and pEGFP pDNA (1.0 $\mu\text{g}/\text{well}$, dissolved in 0.01 M PBS) under $+/-$ charge ratio of 5. The medium was replaced with serum-free medium and the lipoplex solution were added and incubated for another 4 h with lipofectamine 2000 as the reference. The medium was then replaced with 200 μL complete culture medium (with 10% FBS) and cultured (37 °C, 5% CO_2) for an additional 20 h. The GFP fluorescence was observed and recorded on a Nikon Ti-S inverted fluorescence microscope.

4.12. Intracellular localization of the Cy3-labeled DNA enveloped lipoplexes

HeLa and COS-7 cells were seeded into 6-well microplates (4×10^5 cells/well in 1 mL DMEM medium with 10% FBS), and incubated at 37 °C under 5% CO_2 for 24 h. pDNA was pre-labeled with a red-fluorescent agent Cy3 by a Label IT[®] Tracker[™]

Cy3-labeling kits,³⁸ then Cy3-labeled pEGFP-N1 DNA complexed with sterol-based cationic lipids and bPEI-25k were added into each well at the +/– charge ratio about 5. For fluorescence imaging, HeLa cells were washed with 1× PBS for three times to eliminate fluorescence background after 4 h incubation, the cells were fixed with 4% paraformaldehyde in 0.12 M phosphate buffer (pH 7.2) for 10 min, and washed three times with 1× PBS. Furthermore, cell stains DAPI (working concentration 100 ng/mL) and LysoTracker (working concentration 500 ng/mL) were added to stain cell nuclei and lysosome, respectively. After 15 min incubation, the HeLa cells were washed with 1× PBS for three times and the fluorescent images were recorded on Nikon Ti-S invert fluorescence microscopy. Similarly, the COS-7 cells were washed with 1× PBS for three times after incubated with the Cy3-DNA enveloped lipoplexes for 4 h, and was directly observed and recorded on Nikon Ti-S invert fluorescence microscopy.

Acknowledgements

The authors thank partially from National Science Foundation of China (21174160 and 21002116), and specific science foundation of Youth Innovation Promotion Association (YIPA 2011) for their financial supports.

Supplementary data

Supplementary data associated with this article can be found, in the online version, at <http://dx.doi.org/10.1016/j.bmc.2013.08.047>.

References and notes

- Guo, X.; Szoka, F. C. *Acc. Chem. Res.* **2003**, *36*, 335.
- Niidome, T.; Huang, L. *Gene Ther.* **2002**, *9*, 1647.
- Lv, H.; Zhang, S.; Wang, B.; Cui, S.; Yan, J. *J. Controlled Release* **2006**, *114*, 100.
- Morille, M.; Passirani, C.; Vonarbourg, A.; Clavreul, A.; Benoit, J. P. *Biomaterials* **2008**, *29*, 3477.
- Karmali, P. P.; Kumar, V. V.; Chaudhuri, A. J. *Med. Chem.* **2004**, *47*, 2123.
- Zhang, J.; Fan, H.; Levorse, D. A.; Crocker, L. S. *Langmuir* **2011**, *27*, 9473.
- Kedika, B.; Patri, S. V. *Bioconjugate Chem* **2011**, *22*, 2581.
- Zhang, J.; Fan, H.; Levorse, D. A.; Crocker, L. S. *Langmuir* **2011**, *27*, 1907.
- Bajaj, A.; Kondaiah, P.; Bhattacharya, S. *Bioconjugate Chem* **2007**, *18*, 1537.
- Bajaj, A.; Kondaiah, P.; Bhattacharya, S. *J. Med. Chem.* **2008**, *51*, 2533.
- Bajaj, A.; Kondiah, P.; Bhattacharya, S. *J. Med. Chem.* **2007**, *50*, 2432.
- Kolb, H. C.; Sharpless, K. B. *Drug Discovery Today* **2003**, *8*, 1128.
- Amblard, F.; Cho, J. H.; Schinazi, R. F. *Chem. Rev.* **2009**, *109*, 4207.
- Haenni, K. D.; Leigh, D. A. *Chem. Soc. Rev.* **2010**, *39*, 1240.
- Golas, P. L.; Matyjaszewski, K. *Chem. Soc. Rev.* **2010**, *39*, 1338.
- Franc, G.; Kakkar, A. K. *Chem. Soc. Rev.* **2010**, *39*, 1536.
- Johnson, J. A.; Finn, M. G.; Koberstein, J. T.; Turro, N. J. *Macromol. Rapid Commun.* **2008**, *29*, 1052.
- Gramlich, P. M. E.; Wirges, C. T.; Manetto, A.; Carell, T. *Angew. Chem., Int. Ed.* **2008**, *47*, 8350.
- Lutz, J. F.; Zarafshani, Z. *Adv. Drug Deliv. Rev.* **2008**, *60*, 958.
- Hong, V.; Steinmetz, N. F.; Manchester, M.; Finn, M. G. *Bioconjugate Chem.* **2010**, *21*, 1912.
- Kele, P.; Li, X.; Link, M.; Nagy, K.; Herner, A.; Lorincz, K.; Beni, S.; Wolfbeis, O. S. *Org. Biomol. Chem.* **2009**, *7*, 3486.
- O'Mahony, A. M.; Godinho, B. M. D. C.; Ogier, J.; Devocelle, M.; Darcy, R.; Cryan, J. F.; O'Driscoll, C. M. *ACS Chem. Neurosci.* **2012**, *3*, 744.
- Barnard, A.; Posocco, P.; Pricl, S.; Calderon, M.; Haag, R.; Hwang, M. E.; Shum, V. W. T.; Pack, D. W.; Smith, D. K. *J. Am. Chem. Soc.* **2011**, *133*, 20288.
- Zhang, K.; Wang, Y.; Yu, A.; Zhang, Y.; Tang, H.; Zhu, X. X. *Bioconjugate Chem.* **2010**, *21*, 1596.
- Li, C.; Lavigne, C.; Zhu, X. X. *Langmuir* **2011**, *27*, 11174.
- Budker, V.; Jaafari, M. R.; Szoka, F. C., Jr. *Angew. Chem., Int. Ed.* **2009**, *48*, 4146.
- Gao, X.; Huang, L. *Biochem. Biophys. Res. Commun.* **1991**, *179*, 280.
- Budker, V.; Gurevich, V.; Hagstrom, J. E.; Bortzov, F.; Wolff, J. A. *Nat. Biotechnol.* **1996**, *14*, 760.
- Fletcher, S.; Ahmad, A.; Price, W. S.; Jorgensen, M. R.; Miller, A. D. *ChemBioChem* **2008**, *9*, 455.
- Kim, B.-K.; Bae, Y. U.; Doh, K. O.; Hwang, G. B.; Lee, S.-H.; Kang, H.; Seu, Y. B. *Bioorg. Med. Chem. Lett.* **2011**, *21*, 3734.
- Medvedeva, D. A.; Maslov, M. A.; Serikov, R. N.; Morozova, N. G.; Serebrennikova, G. A.; Sheglov, D. V.; Latyshev, A. V.; Vlassov, V. V.; Zenkova, M. A. *J. Med. Chem.* **2009**, *52*, 6558.
- Maslov, M. A.; Morozova, N. G.; Chizhik, E. I.; Rapoport, D. A.; Ryabchikova, E. I.; Zenkova, M. A.; Serebrennikova, G. A. *Carbohydr. Res.* **2010**, *345*, 2438.
- Biswas, J.; Bajaj, A.; Bhattacharya, S. *J. Phys. Chem. B* **2010**, *115*, 478.
- Bhattacharya, S.; Biswas, J. *Langmuir* **2009**, *26*, 4642.
- Jones, S. P.; Gabrielson, N. P.; Pack, D. W.; Smith, D. K. *Chem. Commun.* **2008**, 4700.
- Ghosh, A.; Mukherjee, K.; Jiang, X.; Zhou, Y.; McCarroll, J.; Qu, J.; Swain, P. M.; Baigude, H.; Rana, T. M. *Bioconjugate Chem.* **2010**, *21*, 1581.
- Guo, X. D.; Tandiono, F.; Wiradharma, N.; Khor, D.; Tan, C. G.; Khan, M.; Qian, Y.; Yang, Y. Y. *Biomaterials* **2008**, *29*, 4838.
- Sheng, R.; Luo, T.; Zhu, Y.; Li, H.; Sun, J.; Chen, S.; Sun, W.; Cao, A. *Biomaterials* **2011**, *32*, 3507.
- Cline, L. L.; Janout, V.; Fisher, M.; Juliano, R. L.; Regen, S. L. *Bioconjugate Chem.* **2011**, *22*, 2210.
- Shiraishi, T.; Nielsen, P. E. *Bioconjugate Chem.* **2012**, *23*, 196.
- Gruneich, J. A.; Diamond, S. L. *J. Gene Med.* **2007**, *9*, 381.
- Gruneich, J. A.; Price, A.; Zhu, J.; Diamond, S. L. *Gene Ther.* **2004**, *11*, 668.
- Donald, J. R.; Wood, R. R.; Martin, S. F. *ACS Comb. Sci.* **2012**, *14*, 135.
- Ichikawa, S.; Ueno, H.; Sunadome, T.; Sato, K.; Matsuda, A. *Org. Lett.* **2013**, *15*, 694.
- Sheng, R. L.; Luo, T.; Zhu, Y. D.; Li, H.; Cao, A. *Macromol. Biosci.* **2010**, *10*, 974.
- Rehman, Z. u.; Zuhorn, I. S.; Hoekstra, D. J. *Controlled Release* **2013**, *166*, 46.
- LaManna, C. M.; Lusic, H.; Camplo, M.; McIntosh, T. J.; Barthelemy, P.; Grinstaff, M. W. *Acc. Chem. Res.* **2012**, *45*, 1026.
- Kono, K.; Ikeda, R.; Tsukamoto, K.; Yuba, E.; Kojima, C.; Harada, A. *Bioconjugate Chem.* **2012**, *23*, 871.
- Khatun, U. L.; Gayen, A.; Mukhopadhyay, C. *Chem. Phys. Lipids* **2013**, *170*, 8.
- Maggi, F.; Ciccarelli, S.; Diociaiuti, M.; Casciaroli, S.; Masci, G. *Biomacromolecules* **2011**, *12*, 3499.
- Bryant, G.; Thomas, J. C. *Langmuir* **1995**, *11*, 2480.
- Mindemark, J.; Tabata, Y.; Bowden, T. *Macromol. Biosci.* **2012**, *12*, 840.
- Beyerle, A.; Irmiler, M.; Beckers, J.; Kissel, T.; Stoeger, T. *Mol. Pharm.* **2010**, *7*, 727.
- Zollner, G.; Marschall, H. U.; Wagner, M.; Trauner, M. *Mol. Pharm.* **2006**, *3*, 231.
- Sun, J.; Luo, T.; Sheng, R.; Li, H.; Chen, S.; Hu, F.; Cao, A. *Macromol. Biosci.* **2013**, *13*, 35.
- Bae, Y. U.; Kim, B. K.; Park, J. W.; Seu, Y. B.; Doh, K. O. *Mol. Pharm.* **2012**, *9*, 3579.
- Paryzek, Z.; Joachimiak, R.; Piasecka, M.; Pospieszny, T. *Tetrahedron Lett.* **2012**, *53*, 6212.
- Dykes, G. M.; Brierley, L. J.; Smith, D. K.; McGrail, P. T.; Seeley, G. J. *Chem. Eur. J.* **2001**, *7*, 4730.